Mechanics and Mechanical Engineering
Vol. 15, No. 4 (2011) 53–60
© Technical University of Lodz

The Mathematical Description of the Robot for the Tank Inspection

Mariusz Giergiel
Tomasz Buratowski
Piotr Małka
AGH University of Science and Technology
Department of Robotics and Mechatronics
giergiel@agh.edu.pl
tburatow@agh.edu.pl
piotr.malka@gmail.com

Krzysztof Kurc
Rzeszow University of Technology
Department of Robotics and Mechatronics
kkurc@prz.edu.pl

Received (18 December 2011)
Revised (19 January 2012)
Accepted (5 February 2012)

The paper presents the project of tank inspection robot. In order to discuss the designing process, algorithm of design has been provided. There are four design stages: the analysis of the construction problem, the synthesis, testing/improving robot's construction and finally testing it. First stage of project process is divided into constructive and imitative analysis. Constructive analysis means searching for still not existing solutions of robots and detection methods. In this paper we concentrate only on constructive analysis.

Keywords: Mobile robot, inspection robot, robot for tanks inspection, underwater robot

1. Description of the robot systems and inspection environment

Most of existing inspection robots are designed for metal tanks – they are equipped with magnetic wheels or magnetic caterpillar tracks in order to move on vertical walls. In most cases they are designed to look for corrosion of metal elements or damages in welded connections between metal structures. The general problem is that in most cases of inspection procedure, tanks should be empty in order to build special scaffolds. This scaffolds allow inspectors to get to hard accessible places inside the tank. Because such procedure lasts even one month, the tank is excluded from usage. It has negative influence on the budget of the enterprise which has a duty to provide such inspections periodically. It was essential to obtain some

technical data of storage tanks. On the basis of 2D drawings, 3D documentation has been created using CATIA application. Analysis of 2D and 3D technical data will have huge influence on construction of inspection robot. In Fig. 1 we can see an example of storage tank (3D model created in CATIA).

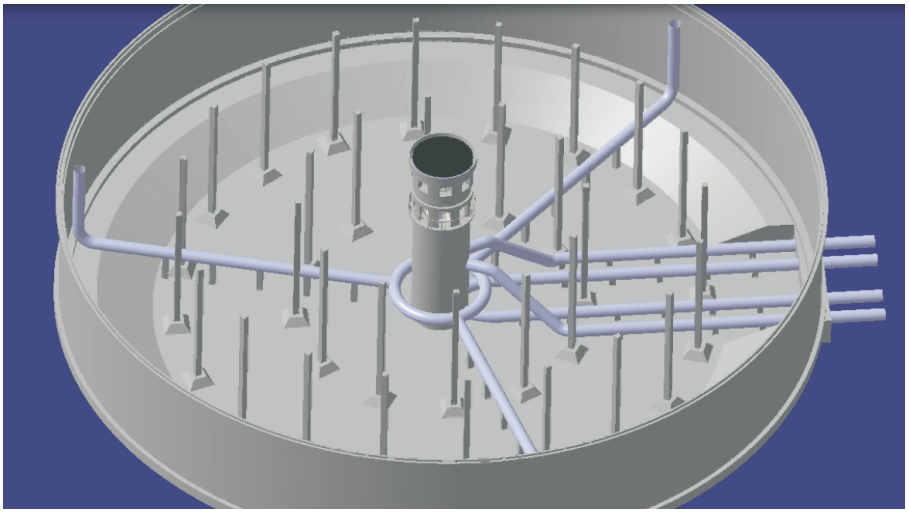

Figure 1 Three dimensional model of the storage tank

It's a reinforced–concrete building with diameter approximately 30 [m]. The roof of tank is supported by two circles of metal columns. There is the so called "central column" in the center of the tank. There are also metal pipes with diameter 0,5 [m] supported by pillars (height 0.5[m]). Dimensions of robot have been assumed relatively small (max. length 0,7[m]). It should get to hard to access places. Also it should be light in order to be easily transported by humans. It's essential to say, that robot will check condition of walls. It can search for any damages in concrete using such a detection methods as checking level of carbonatization, looking for corrosion of metal structures and searching for macro cracks on the walls. There is a need that the robot should operate underwater in order to examine the bottom of the tank and it's walls. The proposed construction of the robot is a modular device. The main idea of it is to simplify this construction as much as possible to create a robust and fully functional inspection unit (Fig. 2).

The robotized system required two units. The main unit is responsible for the large distance movements inside the liquid or a dry tank and is equipped with tracks. The whole robot is designed on the basis of piped framework which provides lightness and stiffness. It's simplicity has influence on low costs of material and manufacturing. Piped modules can be easily changed, if there is no sufficient place inside a robot. Also geometry can be easily changed, especially at the stage of prototyping.

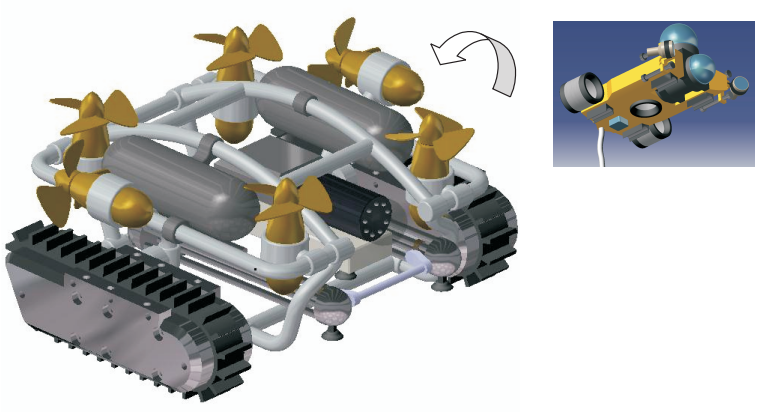

Figure 2 The model of the inspection mobile robotized system

Piped framework allows easy connections. We can mount other modules such as helical drive, lights, tracks etc. Piped framework also allows easy transportation– we can just grab the frame and – if this is necessary – easily detach some parts (i.e. tracks). Tracks allow the robot to move especially on bottom of the tank. Helical drive with optional ballast tanks enables freely motion in liquid. The whole robot is supplied and controlled via cables from safe place outside of storage tank. The second unit is a robotized probe attached to the main robot by the wire. This robot is responsible for inspection and diagnostics of the walls. This robot is designed for short distances an is equipped with two cameras pan/tilt Vivotek PZ7111 and inspection JAI BM–500 GE + Goyo 9 [mm] Lens. All cameras are packed into waterproof housings. Lasers are packed into waterproof housings with adjustable mounts to ensure parallelism between beams. Lights are fixed to the robot by brackets which can be rotated to find the best angle. The homing camera is used only for docking and it should see a lit target on the main robot.

2. Kinematics description of the main robot

On the basis of the previous assumptions the robot moves on caterpillars. The movement of the any point of the caterpillars is connected with composition of two motions [1] (Fig. 3 and Fig. 4)

The first motion is connected with relative motion according to the y_0, z_0 system of coordinates, while the second is connected with the drift motion relative to the stationary y, z system of coordinates.

The first motion is connected with relative motion according to the y_0, z_0 system of coordinates, while the second is connected with the drift motion relative to the stationary y, z system of coordinates. The absolute velocity (3) of any point on the track perimeter is equal to the geometric velocity of the drift and relative velocity (1, 2) [1].

$$V_{by} = V_u + V_t cos\varphi \tag{1}$$

$$V_{bz} = V_t sin\varphi \tag{2}$$

$$V_b = \sqrt{V_{by}^2 + V_{bz}^2} = \sqrt{V_u^2 + V_t^2 + 2V_u V_t cos\varphi} \tag{3}$$

where:

V_u – drify velocity;

V_t – relative velocity of the any point on the on the track perimeter;

V_b – absolute velocity of the point on the track perimeter;

φ – the angle between the velocities V_t and V_u.

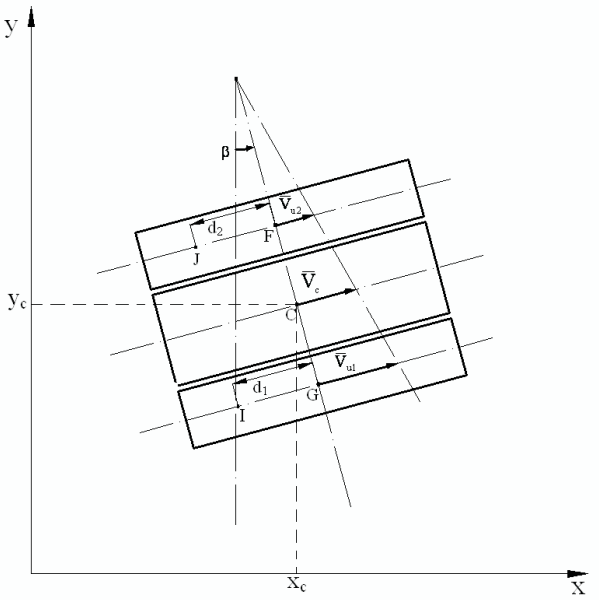

Figure 3 The simplified caterpillar model

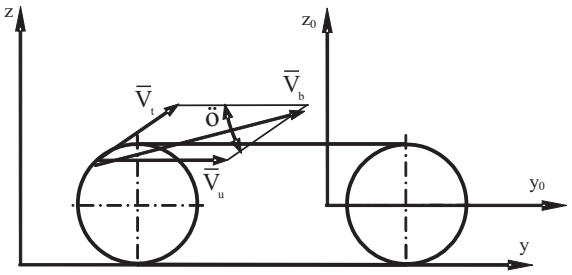

Figure 4 The frame rotation scheme

When there is movement of the carrier section of the track relative to the ground slip phenomenon occurs. Slip Track influenced mainly by the following factors: ground properties, occurring driving force, type and deployment of the clutches of the track.

Existing in the caterpillar system, the driving force causes the shear forces on the ground. Relationship between the common factors can be determined by the equation [1]:

$$P_n = 10^6 b \int_0^L \tau_x dx \tag{4}$$

where:

P_n – driving force;

b – track width;

L – track carrier segment length;

τ_x – shear stress in the soft ground.

The maximum shear stress in the soft ground defines a Coulomb model [2]:

$$\tau_{\max} = c + \mu_0 \sigma = c + \sigma tg\rho \tag{5}$$

where:

ρ – internal friction angle of the ground particles

σ – compressive stresses in the ground

μ_0 – friction coefficient between the ground particles together

c – density of the ground.

The formula for the shear stress depends on the deformation, based on the mathematical analogy between the course of the curves of shear stress and the course of the damped oscillation amplitude of the curve gave Bekker [1], they have the form(12, 13):

$$\tau_x = (c + \sigma tg\rho) \times \frac{e^{(-K_2+\sqrt{K_2^2-1})K_1\Delta l_x} - e^{(-K_2-\sqrt{K_2^2-1})K_1\Delta l_x}}{Y_{\max}} [MPa] \tag{6}$$

where:

Y_{max} – The maximum value of the expression given in the numerator fraction

Δl_x – deformation of the ground layer at x, caused by slipping, parallel to the ground

K_1 – coefficient of the ground deformation during the shearing

K_2 – coefficient characterizing the curve $\tau = f(s)$.

Assuming that, in the course of deformation parallel to the ground is linear, these deformation can be expressed by the formula:

$$\Delta l_x = x s_b \tag{7}$$

where:

s_b – slip calculated from formulas (4) and (6);

x – distance from the point for which the slip is calculated to the point of contact with the ground of track, the largest slip occurs for $x = L$.

On the bases of the description connected with the contact of the track with the ground it is possible to describe the rotation of our robot in the x,y system of

coordinates, it is necessary to assume the characteristic point of the robot C. The scheme of robot motion has been presented in Fig. 4. The velocity components of point C can be written as, after extension by angular velocity of the frame we receive kinematics equations in the form with allow to solve forward kinematics problem [5, 6]:

$$\dot{x}_C = \frac{r\dot{\alpha}_1(1-s_1) + r\dot{\alpha}_2(1-s_2)}{2}\cos\beta \tag{8}$$

$$\dot{y}_C = \frac{r\dot{\alpha}_1(1-s_1) + r\dot{\alpha}_2(1-s_2)}{2}\sin\beta \tag{9}$$

$$\dot{\beta} = \frac{r\dot{\alpha}_2(1-s_2) - r\dot{\alpha}_1(1-s_1)}{H} \tag{10}$$

In order to achieve the desired trajectory it is necessary to solve the inverse kinematics problem, on the basis of dependence (8, 9) and (10) the inverse kinematics equations have been presented in the following form, where H is a distance between the axes of the tracks:

$$V_C = \sqrt{\dot{x}_C^2 + \dot{y}_C^2} \tag{11}$$

$$\dot{\alpha}_1 = \frac{V_C - 0,5\dot{\beta}H}{r(1-s_1)} = \frac{1}{264} = \frac{264(V_C - 0,5\dot{\beta}H)}{r\left(1 - \frac{(n-1)\Delta l'}{L}\right)} \tag{12}$$

$$\dot{\alpha}_2 = \frac{V_C + 0,5\dot{\beta}H}{r(1-s_2)} = \frac{264(V_C + 0,5\dot{\beta}H)}{r\left(1 - \frac{(n-1)\Delta l'}{L}\right)} \tag{13}$$

This kinematic equations allow to control the position and orientation of the robot and to trace desired trajectory.

3. Dynamics description of the main robot

In the dynamics description we expand descriptions of the robot on forces acting but still considering the some characteristic points on the structure [2] (Fig. 5).

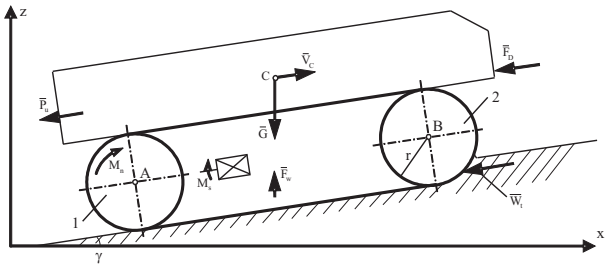

Figure 5 The dynamic model of the robot

The dynamic description of the robot is based on energetic method based on Lagrange equations. In order to avoid modeling problems connected with decoupling Lagrange multipliers Maggi equations are used. The final form of the dynamic motion equations based on Maggi formalism have been presented as follows [3, 4, 7, 8]:

$$\begin{aligned}
&\left(\frac{r}{2}\left[\ddot{\alpha}_1(1-s_1)+\ddot{\alpha}_2(1-s_2)\right]\cos\gamma\right)(m_R+2m)\,\frac{1}{2}r\,(1-s_1)\cos\gamma \\
&\left(\frac{r}{2}\left[\ddot{\alpha}_1(1-s_1)+\ddot{\alpha}_2(1-s_2)\right]\sin\gamma\right)(m_R+2m)\,\frac{1}{2}r\,(1-s_1)\sin\gamma+I_y\ddot{\alpha}_1 \qquad (14)\\
&M_{s1}\eta i+(-0,5P_u-0,5F_D-0,5G\sin\gamma+0,5F_w\sin\gamma-0,5W_{t1})\,r\,(1-s_1) \\
&\left(\frac{r}{2}\left[\ddot{\alpha}_1(1-s_1)+\ddot{\alpha}_2(1-s_2)\right]\cos\gamma\right)(m_R+2m)\,\frac{1}{2}r\,(1-s_2)\cos\gamma \\
&\left(\frac{r}{2}\left[\ddot{\alpha}_1(1-s_1)+\ddot{\alpha}_2(1-s_2)\right]\sin\gamma\right)(m_R+2m)\,\frac{1}{2}r\,(1-s_2)\sin\gamma+I_y\ddot{\alpha}_2 \qquad (15)\\
&M_{s2}\eta i+(-0,5P_u-0,5F_D-0,5G\sin\gamma+0,5F_w\sin\gamma-0,5W_{t2})\,r\,(1-s_2)
\end{aligned}$$

where:

α_1 – angle of rotation for wheel 1, α_2 – angle of rotation for wheel 2,
m_R – frame mass, m – track mass, P_u – ulling force, F_w – hydrostatic force,
W_t – the force of resistance of the rolling track,
F_D – hydrostatic resistance force, I_y – inertia moment for the robot frame,
s_1 – skid for wheel 1, s_2 – skid for wheel 2, G – gravity force, η – efficiency.

4. Simulation on the basis of the robot description

With the use of kinematics and dynamics description of the robot the simulations have been carried out in order to fit construction parameters to optimal work conditions by the robot. In many cases the work environment of the inspection robot is not limited to horizontal surfaces. Sometimes the robot has to overcome the height difference and, therefore, to obtain a more comprehensive analysis of the robot's movement must also be performed in case of motion on the hill.

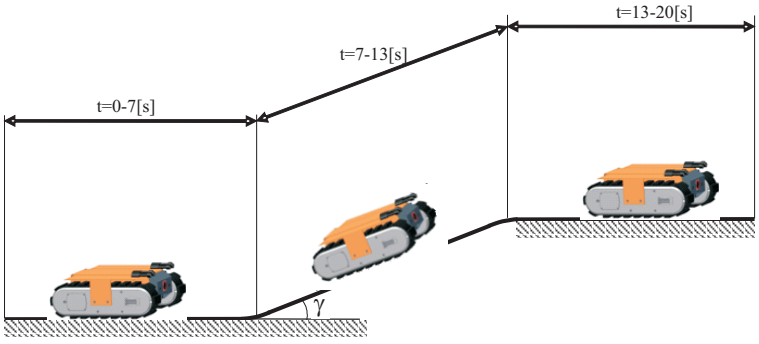

Figure 6 The straight trajectory assumed for the simulation

In the analyzed case the robot moves on the ground with a slope $\gamma = 20^o$ (Fig. 6) and $V_C = 0{,}15$ [m/s], where the track carrier segment length is equal $L = 0{,}322$ [m], the quantity of clutches on truck equals $n = 9$, $\Delta l^{'} = 0{,}0005$ [m] the deformation of the clutch, the radius of the driving wheel of truck $r = 0{,}05$ [m] and the distance $H = 0{,}306$ [m]. After assumption of the velocity of characteristic point C we are receive the kinematic parameters as follows:

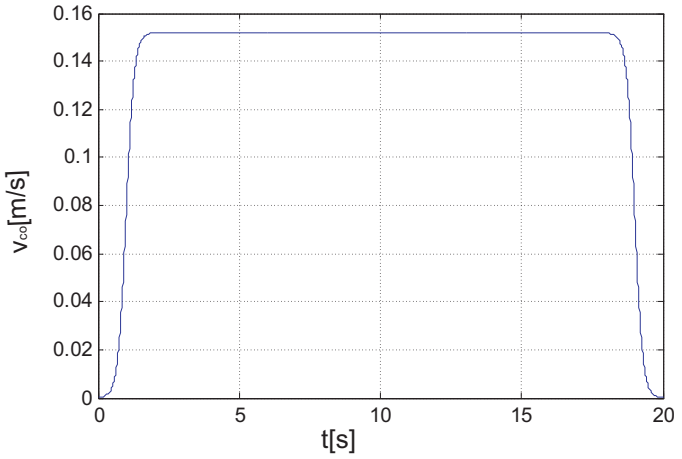

Figure 7 Calculated velocity of the point C

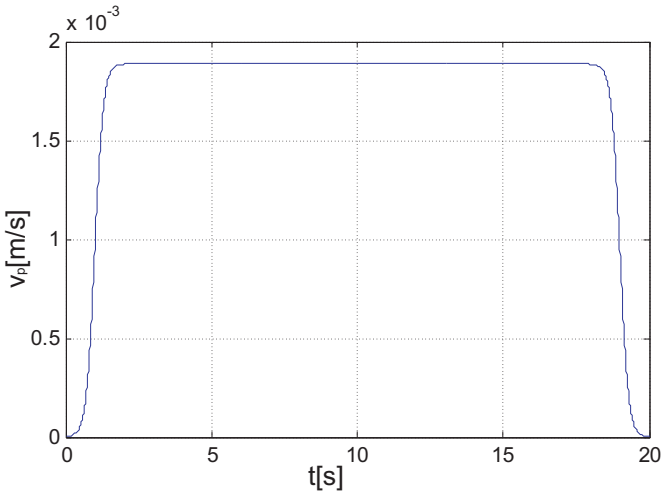

Figure 8 The skid velocity

As can be observed, for the simulation, for ever–greater inflicted on a single horizontal ground deformation, slip velocity increases its value (Fig. 7, Fig. 8). The velocity of point C shell obtain increasing value to ensure the speed of the set point. However, this speed increase is in fact limited by the driving system (speed, power the drive motor), which leads to the fact that the robot starts moving with lower speed ever lost to the slip velocity.

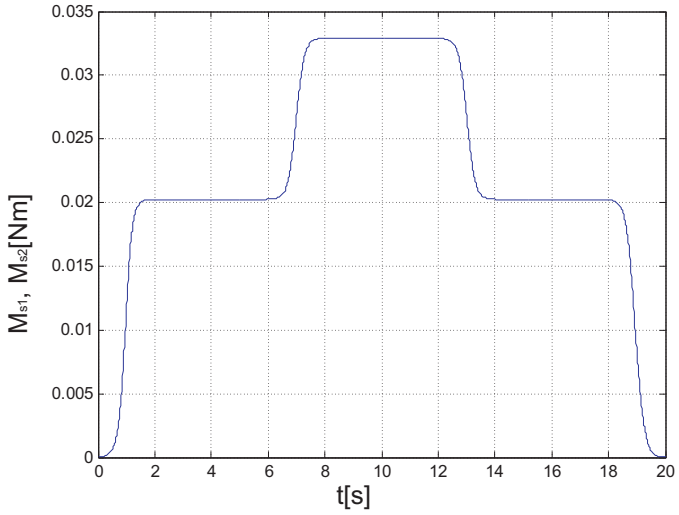

Figure 9 The Driving moments before gearbox

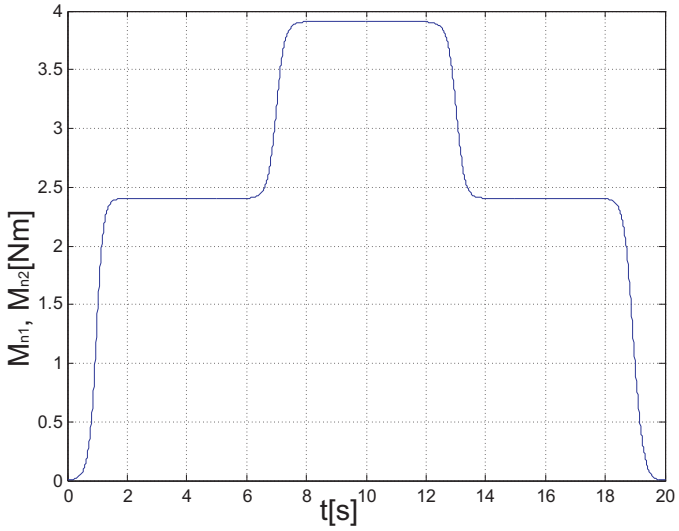

Figure 10 The Driving moments after gearbox

In the dynamics simulation (Fig. 9 and Fig. 10) we receive time courses in which during the robot motion, after a start–up and determining the speed, driving moments have constant value. Change in the moments happens when the robot encounters a hill on its way, and must overcome it with the same speed.

When the robots has driven down the hill the value of the moments return to the previous value and then decline to zero in the 20 [s] of recording time when the robot stops.

5. Summary

The analysis of the kinematics and dynamics and motion simulation takes into account factors such as slipping track–dependent deformation of the substrate and claws, strength, buoyancy robot located in the liquid, the hydrodynamic resistance force depending on the environment in which the robot works and the strength of the rolling resistance of track. This approach will be used for more detailed analysis taking into account additionally the turning of the robot. This will also be necessary during the identification and control this type of object.

Acknowledgments

The research is supported from budget resources by NCBIR as the project N R03–0057–10.

References

[1] **Burdziński, Z.**: Teoria ruchu pojazdu gąsienicowego, *Wydawnictwa Komunikacji i Łączności*, Warszawa, **1972**.

[2] **Dajniak, H.**: Ciągniki teoria ruchu i konstruowanie, *Wydawnictwa Komunikacji i Łączności*, Warszawa, **1985**.

[3] **Żylski, W.**: Kinematyka i dynamika mobilnych robotów kołowych, *Oficyna Wydawnicza Politechniki Rzeszowskiej*, Rzeszów, **1996**.

[4] **Trojnacki, M.**: Modelowanie i symulacja ruchu mobilnego robota trzykołowego z napędem na przednie koła z uwzględnieniem poślizgu kółjezdnych, *Modelowanie Inżynierskie*, vol. 10, No 41, p. 411–420, ISSN 1896–771X, Gliwice, **2011**.

[5] **Chodkowski, A. W.**: Badania modelowe pojazdów gąsienicowych i kołowych, *Wydawnictwa Komunikacji i Łączności*, Warszawa, **1982**.

[6] **Chodkowski, A. W.**: Konstrukcja i obliczanie szybkobieżnych pojazdów gąsienicowych, *Wydawnictwa Komunikacji i Łączności*, Warszawa, **1990**.

[7] **Giergiel, M. J., Hendzel, Z., and Żylski, W.**: Modelowanie i sterowanie mobilnych robotów kołowych, *PWN*, Warszawa, **2002**.

[8] **Giergiel, J., Hendzel, Z., Żylski, W. and Trojnacki, M.**: Zastosowanie metod sztucznej inteligencji w mechatronicznym projektowaniu mobilnych robotów kołowych, Monografia *KRiDM AGH*, Kraków, **2004**.